



Article

Utility of a Hydrolysate from Overproduced *Paralichthys olivaceus* for Hypertension Treatment: Correlation between Physical Properties and Potent Anti-Hypertensive Activities

Hyo-Geun Lee ¹, Jae-Young Oh ², Dong-Min Chung ³, Min-Young Seo ³, Shin-Jae Park ³, You-Jin Jeon ¹ 
and Bo-Mi Ryu ^{1,*} 

¹ Department of Marine Life Science, Jeju National University, Jeju 63243, Korea; hyogeunlee92@gmail.com (H.-G.L.); youjinj@jejunu.ac.kr (Y.-J.J.)

² Food Safety and Processing Research Division, National Institute of Fisheries Science, Busan 46083, Korea; ojoy0724@korea.kr

³ Shinwoo Corporation. Ltd. 991, Worasan-ro, Munsan-eup, Jinju 52839, Korea; jdm@shinwoocorp.com (D.-M.C.); min086@shinwoocorp.com (M.-Y.S.); sjpark@shinwoocorp.com (S.-J.P.)

* Correspondence: ryu.bomi@gmail.com; Tel.: +82-10-4843-7071

Abstract: Aquacultured fish are the richest natural source of protein. However, their overproduced biomass is often discarded due to production imbalance, causing considerable losses to the fishery industry. Therefore, it is necessary to utilize surplus fish and add value to overproduced fish. We performed complex enzyme-assisted hydrolysis to determine the correlation between its physical characteristics and anti-hypertensive activity in vitro and in vivo using an SHR model. Protamex-Pepsin assisted hydrolysate from *Paralichthys olivaceus* (PO_{ppH}) produced by complex enzyme-assisted hydrolysis contained low-molecular-weight peptides and amino acids with anti-hypertensive activity. PO_{ppH} regulated blood pressure and serum angiotensin II and angiotensin-I-converting enzyme levels, and histological and ultrasound image analysis revealed substantially reduced thickness and diameter of the carotid aorta in the PO_{ppH}-administered SHR group. Therefore, we propose to reduce food loss due to overproduction by utilizing the anti-hypertensive activity and physical properties of PO_{ppH}; the results demonstrate its application as a therapeutic agent.

Keywords: *Paralichthys olivaceus*; enzyme-assisted hydrolysis; spontaneously hypertensive rat



Citation: Lee, H.-G.; Oh, J.-Y.; Chung, D.-M.; Seo, M.-Y.; Park, S.-J.; Jeon, Y.-J.; Ryu, B.-M. Utility of a Hydrolysate from Overproduced *Paralichthys olivaceus* for Hypertension Treatment: Correlation between Physical Properties and Potent Anti-Hypertensive Activities. *Mar. Drugs* **2022**, *20*, 346. <https://doi.org/10.3390/md20060346>

Academic Editor: Hideki Kishimura

Received: 28 April 2022

Accepted: 24 May 2022

Published: 25 May 2022

Publisher's Note: MDPI stays neutral with regard to jurisdictional claims in published maps and institutional affiliations.



Copyright: © 2022 by the authors. Licensee MDPI, Basel, Switzerland. This article is an open access article distributed under the terms and conditions of the Creative Commons Attribution (CC BY) license (<https://creativecommons.org/licenses/by/4.0/>).

1. Introduction

Worldwide, approximately one-third of food produced for human consumption is lost or wasted from farm to table, amounting to around 1.3 billion tons per year [1]. In the United States, more than 35 million tons of food went into landfills in 2018 [2]. Wasted food generates severe changes in the marine and terrestrial environments. COVID-19 has exposed the vulnerabilities of food systems and heightened the need to mitigate food loss and waste, both locally and globally [3]. The Food and Agriculture Organization of the United Nations (FAO) stresses the importance of changing perceptions and providing solutions to food loss and wastage [4].

Paralichthys olivaceus (*P. olivaceus*) or olive flounder, belonging to the genus *Paralichthys*, is frequently found in sandy bottoms at 10–200 m. Based on the global statistics of olive flounder production, Korea is the major producer of olive flounder. In 2007, 77.6% (44,245 t) of the global olive flounder supply came from Korea. Olive flounder is often referred to as the Korean flatfish and has been the topmost aquacultured finfish in Korea over the past few decades [5]. However, the expansion of aquaculture production has created several problems, including rice reduction, high mortality due to various diseases, and a sudden increase in olive flounder production resulted in a considerable decrease in their price in the domestic aquaculture fish market. In 2019, 10,634 t of over-produced olive flounder

was discarded in Jeju, Korea [6]. Earlier studies have shown that overproduction and oversupply lead to a price drop due to an imbalance of demand and supply of fish [6]. Therefore, the utilization and processing of over-produced olive flounders can increase their prices and provide a practical solution to overcome the problems associated with overproduction.

Marine fish-derived protein hydrolysates and peptides have remarkable anti-hypertensive properties [7]. Numerous studies have evaluated the effect of angiotensin-I-converting enzyme (ACE) inhibition in vitro and the anti-hypertensive mechanism underlying the lowering of blood pressure or expansion of blood vessels [8]. Our previous studies reported that a protein hydrolysate of *Paralichthys olivaceus* inhibited ACE activity and lowered systolic and diastolic blood pressure in spontaneously hypertensive rat [9]. This study focused on the biological properties of hydrolysates obtained from single enzyme-assisted hydrolysis of *Paralichthys olivaceus*. However, further studies are needed to determine the correlation between their biological activities and physical characteristics, especially the molecular weight of products obtained from single and complex enzyme-assisted hydrolysis of *Paralichthys olivaceus*.

Garcia et al. reported that products of two-stage protamex-pepsin hydrolysis had higher antioxidant, anti-hypertensive, and anti-inflammatory activities than those obtained by one-step protease hydrolysis [10]. In addition, low-molecular-weight peptides with molecular weights less than 1 kDa have greater mobility and diffusivity than high-molecular-weight molecules [11,12]. The physical and compositional characteristics of these hydrolysates are related to their functionality. In this study, we evaluated the potent anti-hypertensive activities of hydrolysates obtained from single and complex enzyme-assisted hydrolysis of *Paralichthys olivaceus* and determined the correlation between their physical characteristics and anti-hypertensive activities. In addition, by discovering the functionality of hydrolysates, we identified the utility of over-produced fish as a therapeutic agent, thus preventing food loss.

2. Results

2.1. Preparation of PO_pH and PO_{pp}H and Their ACE Inhibitory Activities

Protamex-assisted hydrolysate from *Paralichthys olivaceus* (PO_pH) and protamex-pepsin assisted hydrolysate from *Paralichthys olivaceus* (PO_{pp}H) were prepared to establish the enzyme-assisted hydrolysis method and optimize the antihypertensive activity of PO_pH (Figure 1). As shown in Table 1, the angiotensin-I-converting enzyme (ACE) inhibitory activity of PO_{pp}H was higher than that of PO_pH. The IC₅₀ values of ACE for PO_pH and PO_{pp}H were 127.88 ± 1.32 µg/mL and 103.85 ± 0.97 µg/mL, respectively. These results suggest that ACE inhibition can be increased on the group of complex enzyme-assisted hydrolysis.

2.2. Physical Characterization of PO_pH and PO_{pp}H

The physical properties of PO_pH and PO_{pp}H were determined using LC-MS, SEM, and viscosity analysis. The molecular distributions of PO_pH and PO_{pp}H, summarized in Figure 2A, were found to be widely distributed between 300 and 2399 *m/z*; smaller molecular distributions were observed in PO_{pp}H than PO_pH. The molecular distributions of PO_pH had a maximum of 300–2399 *m/z*, and the molecular distributions in PO_{pp}H ranged from 299–1199 *m/z*. PO_pH mainly had distributions in the range 600–899 *m/z* (36%), whereas PO_{pp}H mainly had distributions in the range, 300–599 *m/z* (47%). The molecular mass results of PO_pH and PO_{pp}H are presented in Figure S1. The average molecular weights of PO_pH and PO_{pp}H determined using MALS revealed that they had molecular masses of 2.101×10^3 g/mol and 8.864×10^2 g/mol, respectively. The surface morphologies of PO_pH and PO_{pp}H were observed using field-emission SEM (FE-SEM). The SEM images are shown in Figure 2B. The SEM images of PO_pH revealed an inconsistent surface and mainly had flattened particles with rough surfaces. A rounded and smooth surface morphology was observed for PO_{pp}H under 1.00 kx magnification. The temperature- and shear-rate-dependent viscosities were analyzed for PO_pH and PO_{pp}H. As shown in Figure 2C, large differences in

viscosity η values were found for PO_pH . However, relatively small differences in viscosity η values were found for $PO_{pp}H$. In addition, the shear-rate-dependent viscosity results revealed that the viscosity η of PO_pH was not detected in the range, $10^0 - 10^1 \text{ s}^{-1}$, and its values gradually increased from 10^2 s^{-1} . The shear-rate-dependent viscosity of $PO_{pp}H$ revealed constant viscosity η values in PO_pH . These results suggest that the temperature- and shear-rate-dependent viscosity characteristics were better maintained in $PO_{pp}H$ than in PO_pH .

Procedures	Additives	Conditions
Store in $-80 \text{ }^\circ\text{C}$	Fish fillet (50 kg)	
↓		
Defrost fish fillet		
↓		
Primary hydrolyzation	Fish fillet (50 kg) Water (500 L) <u>Protamax</u> (50 g) Citric acid	pH 6.0 – 7.0, $50 \text{ }^\circ\text{C}$, 2 h
↓		
Secondary hydrolyzation	Pepsin (50g) Citric acid	pH 3.5, $40 \text{ }^\circ\text{C}$, 2 h
Enzyme inactivation		$95 \text{ }^\circ\text{C}$, 30 min
Filtration		$1 \text{ }\mu\text{m}$ filter
Concentration		$65 \text{ }^\circ\text{C}$, 500 – 600 mmHg
Spray drying	Maltodextrin	
Packing		≤ 80 mesh

Figure 1. Preparation of PO_pH and $PO_{pp}H$.

Table 1. ACE inhibitory activity of PO_pH and $PO_{pp}H$.

	PO_pH	$PO_{pp}H$
ACE inhibitory activity, IC_{50} value (mg/mL)	0.56 ± 0.02	0.43 ± 0.03

2.3. Amino Acid Profiles of PO_pH and $PO_{pp}H$

The amino acid compositions of PO_pH and $PO_{pp}H$ were analyzed, and the results are summarized in Table 2. According to amino acid profiling, PO_pH and $PO_{pp}H$ are composed of 18 amino acids: 12 essential amino acids (histidine; His, arginine; Arg, threonine; Thr, proline; Pro, tyrosine; Try, valine; Val, methionine; Met, isoleucine; Ile, leucine; Leu, phenylalanine; Phe, tryptophan; Trp, lysine; Lys), and 6 non-essential amino acids (cysteine, Cys; aspartic acid, Asp; glutamine, Glu; serine, Ser; glycine, Gly; alanine, and Ala). PO_pH and $PO_{pp}H$ had high levels of Ala, Asp, Glu, Arg, Leu, Lys and all these amino acids were slightly increased with complex enzyme assisted hydrolyzation.

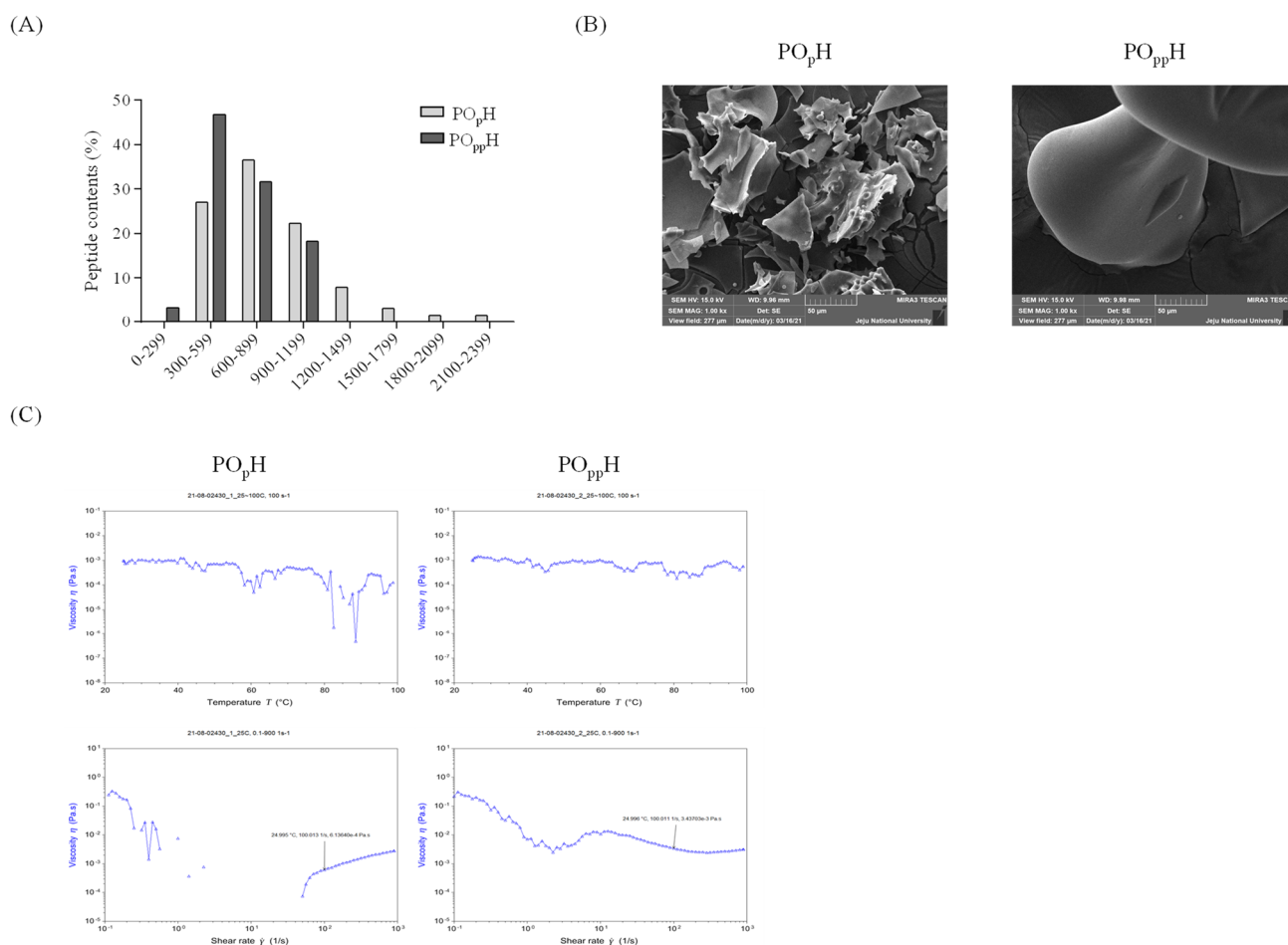


Figure 2. Physical characteristics of PO_pH and PO_{pp}H. (A) Molecular distributions, (B) morphological SEM images, (C) heat and shear activated viscosity.

2.4. PO_{pp}H Reduces SBP and DBP in the SHR Model

The changes in SBP and DBP were evaluated as a measure of the antihypertensive activity of PO_{pp}H during the eight-week experimental period. The initial (week 0) average values of SBP (187.38 ± 12.14 mmHg, $n = 8$) and DPB (126.92 ± 13.07 mmHg, $n = 8$) revealed the rats had hypertension at the beginning of the in vivo study. The blood pressure results presented in Figure 3 reveal that SBP and DBP were considerably downregulated from week 7 to 8 in the groups treated with low and high concentrations of PO_{pp}H compared with those of the SHR groups. L-PO_{pp}H decreased SBP (160.75 ± 13.82 mmHg) and DBP (93.79 ± 23.10 mmHg), and H-PO_{pp}H lowered SBP (156.82 ± 28.34 mmHg) and DBP (81.69 ± 12.25 mmHg) at week 8.

2.5. Effect of PO_{pp}H on Rat Blood Serum Biochemical Indices

To evaluate the antihypertensive effect of PO_{pp}H, blood serum angiotensin II (ANG II) and angiotensin-I-converting enzyme (ACE) levels were analyzed to confirm inhibitory effect of PO_{pp}H on blood ANG II and ACE (Table 3). The ANG II level was remarkably lowered in the L-PO_{pp}H (1729.47 ± 429.05 pg/mL) and H-PO_{pp}H (1445.30 ± 253.30 pg/mL) groups. In addition, ACE levels significantly declined in the H-PO_{pp}H group compared with that in the SHR group. ACE levels considerably decreased to 8.40 ± 0.78 ng/mL in the H-PO_{pp}H group.

Table 2. Amino acid compositions of PO_pH and PO_{pp}H.

Amino Acid	MW of Amino Acids	Concentration (µg/100 µL)	
		PO _p H	PO _{pp} H
Cys	121.160	12.49	14.95
Asp	133.100	97.36	121.21
Glu	147.130	203.10	236.56
Ser	105.090	48.64	59.63
Gly	75.070	47.24	61.93
Ala	89.100	81.76	90.16
His	155.160	5.59	6.79
Arg	174.200	83.67	105.54
Thr	119.120	40.52	48.17
Pro	115.130	31.68	36.96
Tyr	181.190	41.09	47.90
Val	117.150	60.24	69.74
Met	149.210	23.78	25.13
Ile	131.170	56.00	63.44
Leu	131.180	93.77	108.71
Phe	165.190	37.79	44.13
Trp	204.230	18.19	14.79
Lys	146.188	85.64	103.60
Total		1068.55	1259.34

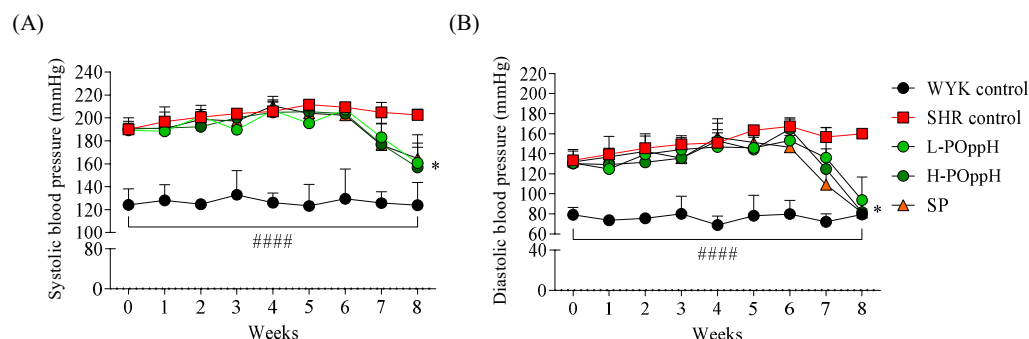


Figure 3. Changes in systolic and diastolic blood pressure after oral administration. (A) Systolic and (B) diastolic blood pressure. (●) WYK control (water); (■) SHR control (water); (●) L-PO_{pp}H (50 mg/kg of PO_{pp}H); (●) H-PO_{pp}H (100 mg/kg of PO_{pp}H); (▲) SP (50 mg/kg of SP). Data are expressed as the mean ± standard deviation (SD), (*n* = 4) in each group. Significant differences were identified at * *p* < 0.05 as compared to the SHR and #### *p* < 0.0001 as compared to WYK control.

Table 3. Effect of PO_{pp}H on serum biochemistry in SHRs.

Groups	ANG II (pg/mL)	ACE (ng/mL)
WYK control	1823.31 ± 294.33 #	8.78 ± 0.87 ###
SHR control	1926.94 ± 266.36	9.98 ± 0.56
L-PO _{pp} H	1729.47 ± 429.05 ***	8.70 ± 0.66 **
H-PO _{pp} H	1445.30 ± 253.30 ****	8.40 ± 0.78 ****
SP	1685.36 ± 374.94 ***	9.01 ± 1.79 **

Significant differences were identified at ** *p* < 0.01, *** *p* < 0.001 and **** *p* < 0.0001, as compared to the SHR control, and # *p* < 0.05 and ### *p* < 0.001, as compared to WYK control.

2.6. Measurement of the Thickness and Ultrasound Imaging of the Carotid Aorta

The effect of PO_{pp}H on the cross-sectional area of the aorta was observed using H&E staining. As shown in Figure 4A, the H&E results revealed a thicker aorta in the SHR group than in the WKY group. However, the thickness of the aorta was significantly reduced in SHRs in the PO_{pp}H groups. In particular, the H-PO_{pp}H group had markedly reduced aorta thickness by 1.38 ± 0.15 -fold relative to the SHR group (1.82 ± 0.12 -fold, ** $p < 0.001$). To determine the diameters of the carotid aorta, ultrasound observation was performed by modifying a method by Jin et al. [13]. As shown in Figure 4B, the carotid aorta images revealed a significantly increase in carotid aorta diameter of H-PO_{pp}H treated group by 1.11 ± 0.03 -fold relative to the SHR group (1.06 ± 0.03 -fold, **** $p < 0.0001$).

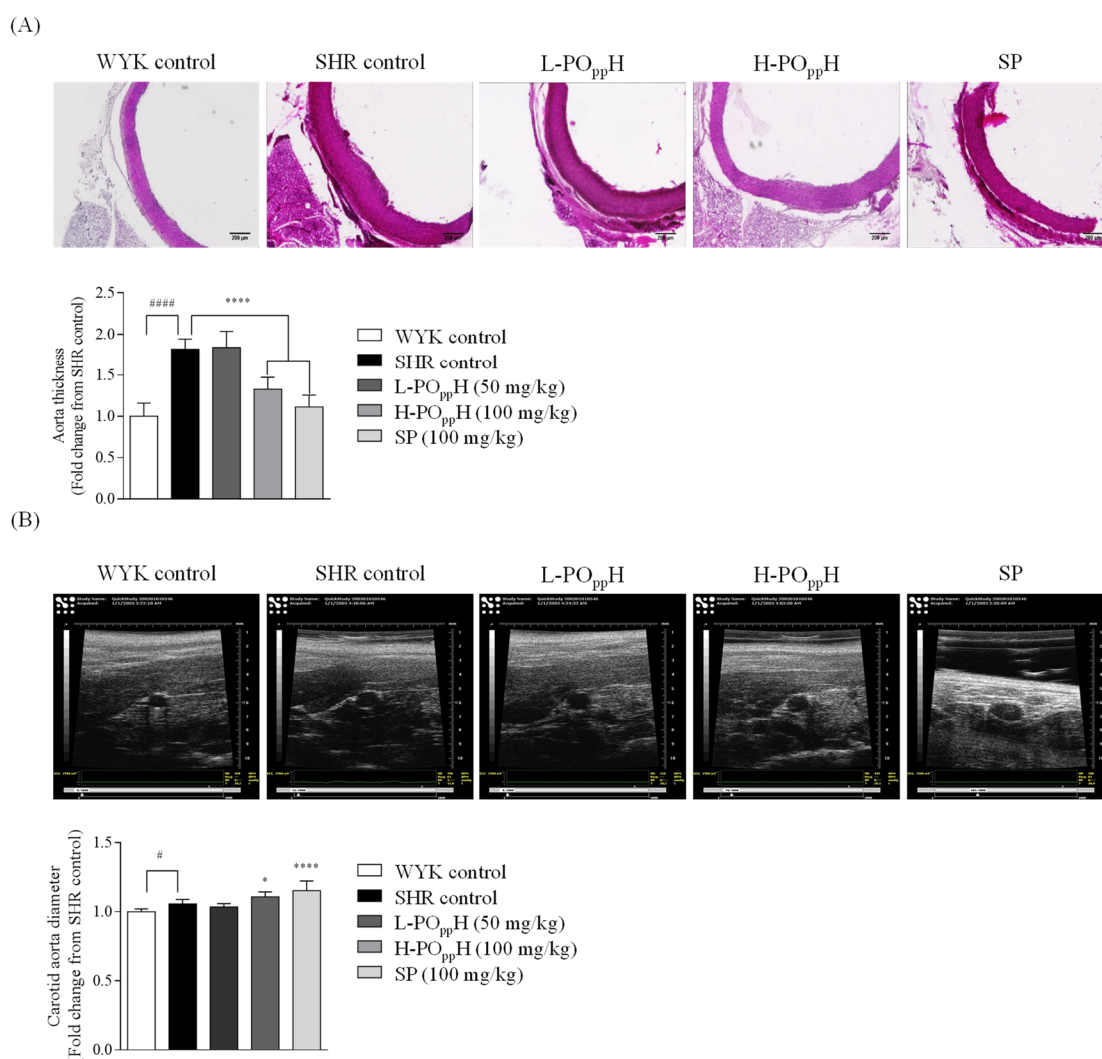


Figure 4. Histologic and ultrasound graphic analysis of the aorta in SHRs. (A) H&E staining images and (B) ultrasound graphic images. Data are expressed as the mean \pm standard deviation (SD), ($n = 3$) in each group. Significant differences were identified at * $p < 0.05$ and **** $p < 0.0001$, as compared to the SHR control, and # $p < 0.05$ and ##### $p < 0.0001$, as compared to WYK control.

3. Discussion

Hypertension is one of the main mediators of cardiovascular diseases [14]. Elevated central blood flow is highly burdensome and induces damage in tissues and organs, including the heart, kidney, brain, and blood vessels, ultimately resulting in organ dysfunction and failure [15]. Katz et al. reported that most patients with end-organ injuries showed a high rate of chronic and acute hypertension [16]. Therefore, the management and initial control of blood pressure (BP) could help minimize the risk of outbreak of hypertension.

Recent research with animals revealed that marine fish hydrolysate and its bioactive peptide have strong angiotensin-I-converting enzyme (ACE) inhibitory activity in vitro and exponentially ameliorate blood pressure [9,17–20]. However, most studies on marine fish hydrolysate have focused on their biological properties and adopted single-enzyme-assisted hydrolysis to collect fish hydrolysates. Furthermore, the relative biological activities of single and complex enzyme-assisted hydrolysates and the subsequent changes in physical characteristics have not been fully investigated. Here, protamex hydrolysis was adopted as a one-step hydrolysis, and two-step protamex-pepsin hydrolysis was performed on fish fillets from *Paralichthys olivaceus* to assess their potent antihypertensive activities depending on changes in their physical characteristics.

The molecular distribution results revealed the presence of relatively low molecular weight peptide in PO_{pp}H compared to that in PO_pH, implying that the low molecular weight peptide was concentrated in PO_{pp}H during the two-step hydrolysis. Further, the average molecular weights of PO_pH and PO_{pp}H were 2.101×10^3 g/mol and 8.864×10^2 g/mol, respectively. Lin et al. reported the increased potency of ACE inhibitory activity and the potential of antihypertensive properties of low molecular weight protein hydrolysates [21]. Morphologic images of PO_pH and PO_{pp}H revealed that the surface morphologies changed during complex enzyme-assisted hydrolysis. The surface of PO_pH showed comparatively irregular patterns and rough surface particles. However, a smooth and rounded surface was observed for PO_{pp}H. The temperature- and shear-rate-dependent viscosity results indicated that the physical characteristics, especially temperature- and shear-rate-dependent viscosity, were highly maintained in PO_{pp}H compared to those in PO_pH. The amino acid compositions of PO_pH and PO_{pp}H showed an increase in the Ala, Asp, Glu, Arg, Leu, Lys in PO_{pp}H relative to that in PO_pH. These results correspond with those of previously published reports on the ACE inhibitory activity of marine fish-derived peptides [9,22,23]. Moreover, the PO_{pp}H contained ACE inhibitory peptides, including Ala and Leu, indicating that PO_{pp}H might have potential antihypertensive properties [24]. Lee et al. reported that the ACE inhibitory activity is closely associated with the degree of enzyme hydrolysis and peptide sequences and their amino acid composition [25]. The physical analysis results indicated that the physical and chemical characteristics changed with two-step hydrolysis. In particular, the low-molecular-weight peptides and antihypertensive amino acids were found to be concentrated by two-step hydrolysis. In addition, PO_{pp}H maintained a constant viscosity under temperature- and shear-rate-dependent conditions. These results suggest that compared with single enzyme-assisted hydrolysis, the complex enzyme-assisted hydrolysis markedly increased the antihypertensive potential by increasing the low molecular peptide and antihypertensive amino acid content.

The in vitro ACE inhibitory activities revealed that ACE inhibition was significantly increased in PO_{pp}H (IC₅₀, 0.43 ± 0.03 mg/mL). Earlier reports by Ko et al. (2016) indicate that the pepsin-assisted hydrolysate from flounder fish showed 50% of ACE inhibition at 1.26 ± 0.14 mg/mL. These results demonstrated the ACE inhibitory activity was increased through the two-step protamex-pepsin enzyme-assisted hydrolysis, thereby influencing the selection of PO_{pp}H for further in vivo animal antihypertensive studies. In vivo, hypertension was successfully induced in the SHR model (SBP: 187.38 ± 12.14 mmHg, DBP: 126.92 ± 13.07 mmHg). WKY rats maintained an SBP of 123.99 ± 14.13 mmHg and a DBP of 79.14 ± 7.20 mmHg during the initial steps of the experiment. During the eight weeks of SBP and DBP monitoring, high SBP and DBP was maintained in the SHR and PO_{pp}H groups from weeks 0 to 6. However, SBP and DBP significantly decreased from week 7 in the H-PO_{pp}H group compared to those in the SHR control group. However, the dose dependent SBP and DBP lowering effect of PO_{pp}H on the SHR model could not be found. Nonetheless, our findings indicate that the critical concentrations of PO_{pp}H on SBP and DBP were 100–200 mg/kg. Based on blood serum analysis, serum angiotensin II (ANG II) and ACE levels were significantly decreased in the PO_{pp}H groups. These results correspond with those of previous reports on ANG II and ACE activation [26,27]. Chappell reported the functions of ANG II and ACE on vasorelaxation in humans [28]. PO_{pp}H was

found to significantly lower SBP and DBP by regulating serum ANG II and ACE levels. Histological analysis indicated that the thickness of the aorta was markedly reduced following H-PO_{pp}H administration. These results correspond with those of Ashkan et al., who demonstrated the relationship between aortic wall thickness and aortic distensibility [29]. Overall, our findings suggest that H-PO_{pp}H could ameliorate hypertension-induced aorta or blood vessel hypertrophy in SHR. Moreover, ultrasound image analysis demonstrated that supplementation with PO_{pp}H remarkably increased the carotid aorta diameter. Collectively, these results imply that the oral administration of PO_{pp}H significantly reduced SBP and DBP by regulating ANG II and ACE levels. Furthermore, the oral administration of PO_{pp}H can reduce the risk of aortic and cardiac hypertrophy.

4. Materials and Methods

4.1. Materials and Chemicals

Commercial protamex was purchased from Novo Co. (Novo Nordisk, Bagsvaerd, Denmark). Pepsin was purchased from Chongqing Jiangxia Biochemistry Pharmaceutical Co., Ltd. (Chongqing, China). The in vitro ACE kit-WST was purchased from Dojindo Inc. (Kumamoto, Japan). Serum angiotensin II (ANG II) and angiotensin-I-converting enzyme (ACE) analysis kits were purchased from LS Bio (Washington, DC, USA). All chemicals and reagents were of analytical grade.

4.2. Preparation of Enzymatic Hydrolysate from *Paralichthys olivaceus*

Paralichthys olivaceus were obtained from a local fish farm on Jeju Island, Korea. The fish were filleted, washed with tap water, and stored at $-80\text{ }^{\circ}\text{C}$. The frozen fish fillet was defrosted, and 50 kg of fish fillet was hydrolyzed with protamex (50 g) for 2 h under optimal conditions (pH 6.00–7.00, $50\text{ }^{\circ}\text{C}$). After protamex-assisted hydrolysis, the pH of hydrolysate of *Paralichthys olivaceus* (PO_pH) was adjusted to 3.50 with citric acid and additional 50 g of pepsin was added. The pepsin-assisted hydrolysis was continued for 2 h under $40\text{ }^{\circ}\text{C}$, after which, the protamex-pepsin were inactivated at $95\text{ }^{\circ}\text{C}$ for 30 min. The mixtures were subsequently filtered (pore size: $1\text{ }\mu\text{m}$), and the filtrate was concentrated in a vacuum concentrator ($60\text{ }^{\circ}\text{C}$, 500–600 mmHg) up to 20 brix. The concentrated solutions were then mixed with maltodextrin and spray-dried under optimal conditions (inlet: 165–180, outlet: 70–90, rpm: 10,000). Thereafter, the spray-dried samples were stored in a freezer at $-20\text{ }^{\circ}\text{C}$ before use. Finally, the resulting protamex-pepsin assisted hydrolysate of *Paralichthys olivaceus* was named as PO_{pp}H (Lot No. SW1K11SA).

4.3. ACE Inhibitory Activity

The ACE inhibitory effect of PO_pH and PO_{pp}H was determined using a commercial ACE assay kit (Dojindo Molecular Technologies, Inc., Kumamoto, Japan), according to the manufacturer's instructions.

4.4. Molecular Distribution Based on Liquid Chromatography-Mass Spectrometry (LC-MS)

LC-MS analysis was performed to derive the molecular weight distributions of PO_pH and PO_{pp}H. The mass spectra were acquired using an UltiMate 3000 system (Dionex, Sunnyvale, CA, USA) coupled with a microQ-TOF III mass spectrometer (Bruker Corporation, 255748, Bremen, Germany). ZORBAX 300SB-C18 ($1.0 \times 150\text{ mm}$, $3.5\text{ }\mu\text{m}$, Agilent) was used as the separation column. The tested samples were directly infused into positive-mode ESI sources at a speed of $100\text{ }\mu\text{L}/\text{min}$. The MS scan range was 200–2000 m/z , and the MS parameters were as follows: capillary voltage, 4500 V; dry temperature: $180\text{ }^{\circ}\text{C}$; funnel 1RF, 400; funnel 2RF, 400; ISCID energy, 0 eV; Hexapole RF, 250; Ion Energy, 5.0 eV; Low Mass, 300 m/z ; Collision Energy, 7 eV; Collision RF, 600; Transfer Time, 80 μs ; and Pre Puls Storage, 10 μs). To measure the molecular weight distributions, distilled water with 0.2% formic acid was used as the mobile phase (A), while acetonitrile containing 0.2% formic acid was used as the stationary phase (B). The tested samples were eluted using a gradient of mobile phase. The tested samples were eluted using a gradient of mobile phase (A) and

stationary phase (B) at a flow rate of 100 $\mu\text{L}/\text{min}$, and the wavelength of detection was 280 nm. The following gradient elution program was employed: 0–4 min, 95:95–5:5 v/v ; 4–5 min, 95:90–5:10 v/v ; 5–25 min, 90:70–10:30 v/v ; 25–30 min, 70:5–30:95 v/v ; 30–40 min, 5:5–95:95 v/v ; and 40–46 min, 5:95–95:5 v/v .

4.5. Determining Average Molecular Weight by Multi-Angle Light Scattering (MALS)

To determine the average molecular weight, MALS analysis was performed using DAWN Heleos II multi-angle light scattering coupled with a Shimadzu HPLC system connected to a PL aquagel-OH MIXED-H (7.5×300 mm, Agilent Technologies, Santa Clara, CA, USA). The analytical sample was dissolved in 500 mM NaCl and filtered through a membrane filter (pore size: 0.22 μm). The filtered samples were subsequently loaded and eluted with 0.5 mol/L NaCl at a flow rate of 0.5 mL/min. The MALS data were analyzed using the ASTRA 6 software (Wyatt Technologies, Santa Barbara, CA, USA).

4.6. Rheometry

A rotational rheometer (ARES-G2, TA Instruments Ltd., Newcastle, DE, USA) was used to assess the temperature–shear rate dependent viscosity of PO_pH and PO_{pp}H . The temperature-dependent viscosities of PO_pH and PO_{pp}H were evaluated at 20, 40, 60, 80, and 100 $^\circ\text{C}$, and the shear-rate-dependent viscosity was measured in the range of 10^{-1} to 10^3 s^{-1} . The following parameters were applied: minimum transducer torque in oscillation: 0.05 N·m; minimum transducer torque in steady shear, 0.1 N·m; maximum transducer torque, 200 mN·m; transducer torque resolution, 1 nN·m; strain resolution at drive motor, 0.04; measuring geometry, 25 mm plate; and measuring Gap, 1 mm.

4.7. Scanning Electron Microscopy (SEM)

Surface morphologies were determined using field emission scanning electron microscopy (FE-SEM; MIRA 3 TESCAN, Brno, Czech Republic) coupled with energy dispersive X-ray spectrometry (EDS). The sample was mounted on circular aluminum stubs, coating the carbon tape. After the sample was pretreated, the stub was introduced into the FE-SEM device, and the surface morphology and structure were analyzed using FE-SEM (SEM HV: 15.0 kV, magnification: 1.00 kx).

4.8. Amino Acid Composition

General amino acid profiles were analyzed using an amino acid auto analyzer coupled with an HPLC system (Waters, Milford, MA, USA) equipped with a Pico-Tag reverse-phase column (3.9×300 mm, pore size: 4 μm). For amino acid analysis, solvent A (140 mM sodium acetate, 6%(v/v) ACN, pH 5.9) and solvent B (60%(v/v) ACN) were used as mobile phases, and gradient separation was performed at a flow rate of 1 mL/min. The amino acids were detected in a Waters 2487 UV detector at 254 nm. Data were analyzed using Waters Empower 2 software. The following gradient elution of solvent A and B was employed: 0–9 min, 100:0–86:14 v/v ; 9–9.2 min, 86:14–80:20 v/v ; 9.2–17.5 min, 80:20–54:46 v/v ; 17.5–17.7 min, 54:46–0:100 v/v ; and 17.7–21 min, 0:100–100:0 v/v .

4.9. Animal Studies

Thirty-two male SHRs and eight male Wistar rats (WKY) (age of rats, 5 weeks old) were purchased from a commercial vendor, Jung Ang Lab Animal Inc. (Seoul, Korea). All animals had free access to tap water and chow diet containing proteins (15.2%), lipids (2.9%), cellulose (4.1%), nitrogen-free extract (60.7%), moisture (12.1%), and mineral ash (5.0%). Rats were housed in a controlled room under optimal temperature (20–22 $^\circ\text{C}$), humidity (40–60%), and a 12:12 light/dark cycle. Animals were allowed to acclimate to the environment for two weeks. Thereafter, the animals were randomly divided into five groups ($n = 8$ in each group): normal control (WYK), negative control (SHR), positive control (sardine peptide (SP)), low (L- PO_{pp}H), and high (H- PO_{pp}H) dosage groups. The L- PO_{pp}H and H- PO_{pp}H mice were orally administered 50 and 100 mg/kg of PO_{pp}H once

daily, respectively. The positive control groups were orally administered 100 mg/kg SP once daily, and the normal and negative control groups were administered 0.9% saline. Systolic blood pressure (SBP) and Diastolic blood pressure (DBP) were monitored weekly using a CODATM tail-cuff blood pressure system (Kent Scientific Corp., Torrington, CT, USA). All experimental rats were sacrificed to retrieve their kidney, heart, and aorta tissues for further histological experiments. The animal study was approved by the International Animal Care and Use Committee (IACUC) of Jeju National University (approval number: 2020-0025, 13 July 2020).

4.10. Blood Serum Profiles

Blood was collected from rat heart via a cardiac puncture using an EDTA-rinsed syringe. Subsequently, the blood was transferred into a heparin-coated blood collection tube. Blood serum was allowed to coagulate for 1 h before centrifugation (3000 rpm, 15 min, 4 °C). Thereafter, the supernatant was carefully collected and stored at −80 °C.

4.11. Histology

Histological analysis was performed by dissecting the rat aorta. The isolated aorta tissues were fixed in 10% formalin solution and dehydrated before embedding in paraffin. Subsequently, the blocks of paraffin-embedded aorta tissue were cut into 3- μ m sections using a tissue processor machine, placed on an albumin-coated slide, and dried at 37 °C for 24 h. Thereafter, the slides were deparaffinized in xylene, stained with hematoxylin and eosin (H&E) staining, and rinsed three times with deionized water. The slides were mounted with DPX mounting solution (Sigma Chemical Co., St. Louis, MO, USA). Histologic images were obtained using Lionheart FX Automated Microscope (BioTek Instruments, Inc., Winooski, VT, USA). The thickness of rat aorta tissues was measured using ImageJ software (version 1.4).

4.12. Ultrasound Image Analysis

SHRs (8 weeks old) were anesthetized with diethyl ether and O₂ gas through a vevo compact anesthesia system. Carotid artery images were observed using the modified methods of Phaeng et al. with a Vevo 770 small animal ultrasound imaging scanner and single-element crystal mechanical imaging transducer (RMV 704; VisualSonics Inc., Toronto, ON, Canada) [30]. The diameter of the carotid aorta was quantified using MATLAB software (Math Works Inc., Natick, MA, USA).

4.13. Statistical Analysis

All measurements were performed in triplicate and are presented as mean \pm standard deviation (SD) using the statistical package, GraphPad Prism (Version 6; GraphPad Software Inc., San Diego, CA, USA). One-way ANOVA with Duncan's test was used to assess differences between the groups. *p*-values in the following limits were considered significant: * *p* < 0.05, ** *p* < 0.01, *** *p* < 0.001, and **** *p* < 0.0001 compared with the negative SHR control group; and # *p* < 0.05, ## *p* < 0.01, ### *p* < 0.001, and #### *p* < 0.0001 compared with the normal WYK control group.

5. Conclusions

In conclusion, our findings revealed that complex enzyme-assisted hydrolysis, similar to two-step protamex-pepsin enzyme-assisted hydrolysis, successfully increased the low molecular weight peptide. Moreover, physical characteristics, such as viscosity, were highly maintained in PO_{pp}H. The oral administration of PO_{pp}H potentially caused SBP and DBP lowering by downregulating angiotensin II and down-regulating of angiotensin-I-converting enzyme levels. Taken together, these results indicate that PO_{pp}H can be utilized as an anti-hypertensive agent. Further, this study provides a rationale for clinical studies on low-molecular-weight peptides from *Paralichthys olivaceus* used as anti-hypertensive func-

tional food or agents. The anti-hypertensive activity of *Paralichthys olivaceus* by-products could minimize the loss of aquaculture fisheries and food waste.

Supplementary Materials: The following supporting information can be downloaded at: <https://www.mdpi.com/article/10.3390/md20060346/s1>, Figure S1: Molecular distributions of POpH and POppH.

Author Contributions: H.-G.L.: Conceptualization, Methodology, Validation, Formal analysis, Investigation, Writing—original draft preparation, Writing—review and editing; J.-Y.O.: Software, Resources; D.-M.C., M.-Y.S. and S.-J.P.: Software, Resources, Data curation; Y.-J.J. and B.-M.R.: Conceptualization, Supervision, Project administration, Funding acquisition. All authors have read and agreed to the published version of the manuscript.

Funding: This research was supported by a part of the project titled ‘Development of functional food products with natural materials derived from marine resources (No. 20170285)’, funded by the Ministry of Oceans and Fisheries, Korea.

Institutional Review Board Statement: The animal study was approved by the International Animal Care and Use Committee (IACUC) of Jeju National University (approval number: 2020-0025, 13 July 2020).

Informed Consent Statement: Not applicable.

Data Availability Statement: Not applicable.

Acknowledgments: This research was supported by a part of the project titled ‘Development of functional food products with natural materials derived from marine resources (No. 20170285)’, funded by the Ministry of Oceans and Fisheries, Korea.

Conflicts of Interest: The authors declare no conflict of interest.

References

1. Liao, F.; Qing, P.; Hou, M.-H. Analysis on the influencing factors of consumers’ wasting food behaviors: Based on the theory of planned behaviors. *Res. Agric. Mod.* **2020**, *41*, 115–124.
2. Zhongming, Z.; Linong, L.; Wangqiang, Z.; Wei, L. *Key Messages on the International Day of Awareness of Food Loss and Waste*; United States Department of Agriculture: Washington, DC, USA, 2021.
3. Rivera-Ferre, M.G.; López-i-Gelats, F.; Ravera, F.; Oteros-Rozas, E.; di Masso, M.; Binimelis, R.; El Bilali, H. The relation of food systems with the COVID19 pandemic: Causes and consequences. *Agric. Syst.* **2021**, *191*, 103134. [[CrossRef](#)]
4. Loboguerrero, A.M.; Campbell, B.M.; Cooper, P.J.; Hansen, J.W.; Rosenstock, T.; Wollenberg, E. Food and earth systems: Priorities for climate change adaptation and mitigation for agriculture and food systems. *Sustainability* **2019**, *11*, 1372. [[CrossRef](#)]
5. Bai, S.C.; Lee, S. Culture of olive flounder: Korean perspective. In *Practical Flatfish Culture and Stock Enhancement*; John Wiley & Sons: Hoboken, NJ, USA, 2010; pp. 156–168.
6. Getu, A.; Misganaw, K.; Bazezew, M. Post-harvesting and major related problems of fish production. *Fish. Aquac. J.* **2015**, *6*, 1000154. [[CrossRef](#)]
7. UG, Y.; Bhat, I.; Karunasagar, I.; Mamatha, B.S. Antihypertensive activity of fish protein hydrolysates and its peptides. *Crit. Rev. Food Sci. Nutr.* **2019**, *59*, 2363–2374.
8. Ishak, N.H.; Shaik, M.I.; Yellapu, N.K.; Howell, N.K.; Sarbon, N.M. Purification, characterization and molecular docking study of angiotensin-I converting enzyme (ACE) inhibitory peptide from shortfin scad (*Decapterus macrosoma*) protein hydrolysate. *J. Food Sci. Technol.* **2021**, *58*, 1–11. [[CrossRef](#)]
9. Oh, J.-Y.; Kim, E.-A.; Lee, H.; Kim, H.-S.; Lee, J.-S.; Jeon, Y.-J. Antihypertensive effect of surimi prepared from olive flounder (*Paralichthys olivaceus*) by angiotensin-I converting enzyme (ACE) inhibitory activity and characterization of ACE inhibitory peptides. *Process Biochem.* **2019**, *80*, 164–170. [[CrossRef](#)]
10. García, J.; Méndez, D.; Álvarez, M.; Sanmartín, B.; Vázquez, R.; Regueiro, L.; Atanassova, M. Design of novel functional food products enriched with bioactive extracts from holothurians for meeting the nutritional needs of the elderly. *LWT* **2019**, *109*, 55–62. [[CrossRef](#)]
11. Ishak, N.; Sarbon, N. A review of protein hydrolysates and bioactive peptides deriving from wastes generated by fish processing. *Food Bioprocess Technol.* **2018**, *11*, 2–16. [[CrossRef](#)]
12. Karoud, W.; Sila, A.; Krichen, F.; Martínez-Alvarez, O.; Bougatef, A. Characterization, surface properties and biological activities of protein hydrolysates obtained from hake (*Merluccius merluccius*) heads. *Waste Biomass Valorization* **2019**, *10*, 287–297. [[CrossRef](#)]
13. Jin, C.; Nam, K.-H.; Paeng, D.-G. Asymmetric pulsation of rat carotid artery bifurcation in three-dimension observed by ultrasound imaging. *Int. J. Cardiovasc. Imaging* **2016**, *32*, 1499–1508. [[CrossRef](#)] [[PubMed](#)]
14. Kjeldsen, S.E. Hypertension and cardiovascular risk: General aspects. *Pharmacol. Res.* **2018**, *129*, 95–99. [[CrossRef](#)] [[PubMed](#)]

15. Hashimoto, J. Central hemodynamics and target organ damage in hypertension. *Tohoku J. Exp. Med.* **2014**, *233*, 1–8. [[CrossRef](#)] [[PubMed](#)]
16. Katz, J.N.; Gore, J.M.; Amin, A.; Anderson, F.A.; Dasta, J.F.; Ferguson, J.J.; Kleinschmidt, K.; Mayer, S.A.; Multz, A.S.; Peacock, W.F. Practice patterns, outcomes, and end-organ dysfunction for patients with acute severe hypertension: The Studying the Treatment of Acute hyperTension (STAT) registry. *Am. Heart J.* **2009**, *158*, 599–606.e1. [[CrossRef](#)] [[PubMed](#)]
17. Chen, J.; Ryu, B.; Zhang, Y.; Liang, P.; Li, C.; Zhou, C.; Yang, P.; Hong, P.; Qian, Z.J. Comparison of an angiotensin-I-converting enzyme inhibitory peptide from tilapia (*Oreochromis niloticus*) with captopril: Inhibition kinetics, in vivo effect, simulated gastrointestinal digestion and a molecular docking study. *J. Sci. Food Agric.* **2020**, *100*, 315–324. [[CrossRef](#)]
18. Fu, W.; Wang, P.; Wu, H.; Zhang, Z.; Zeng, H.; Zhang, Y.; Zheng, B.; Hu, J. Antihypertensive effects of Trichiurus lepturus myosin hydrolysate in spontaneously hypertensive rats. *Food Funct.* **2020**, *11*, 3645–3656. [[CrossRef](#)]
19. Je, J.-G.; Kim, H.-S.; Lee, H.-G.; Oh, J.-Y.; Lu, Y.A.; Wang, L.; Rho, S.; Jeon, Y.-J. Low-molecular weight peptides isolated from seahorse (*Hippocampus abdominalis*) improve vasodilation via inhibition of angiotensin-converting enzyme in vivo and in vitro. *Process Biochem.* **2020**, *95*, 30–35. [[CrossRef](#)]
20. Oh, J.-Y.; Je, J.-G.; Lee, H.-G.; Kim, E.-A.; Kang, S.I.; Lee, J.-S.; Jeon, Y.-J. Anti-Hypertensive Activity of Novel Peptides Identified from Olive Flounder (*Paralichthys olivaceus*) Surimi. *Foods* **2020**, *9*, 647. [[CrossRef](#)]
21. Lin, F.; Chen, L.; Liang, R.; Zhang, Z.; Wang, J.; Cai, M.; Li, Y. Pilot-scale production of low molecular weight peptides from corn wet milling byproducts and the antihypertensive effects in vivo and in vitro. *Food Chem.* **2011**, *124*, 801–807. [[CrossRef](#)]
22. Gu, R.-Z.; Li, C.-Y.; Liu, W.-Y.; Yi, W.-X.; Cai, M.-Y. Angiotensin I-converting enzyme inhibitory activity of low-molecular-weight peptides from Atlantic salmon (*Salmo salar* L.) skin. *Food Res. Int.* **2011**, *44*, 1536–1540. [[CrossRef](#)]
23. Lee, J.K.; Jeon, J.-K.; Byun, H.-G. Antihypertensive effect of novel angiotensin I converting enzyme inhibitory peptide from chum salmon (*Oncorhynchus keta*) skin in spontaneously hypertensive rats. *J. Funct. Foods* **2014**, *7*, 381–389. [[CrossRef](#)]
24. Hong, F.; Ming, L.; Yi, S.; Zhanxia, L.; Yongquan, W.; Chi, L. The antihypertensive effect of peptides: A novel alternative to drugs? *Peptides* **2008**, *29*, 1062–1071. [[CrossRef](#)] [[PubMed](#)]
25. Lee, S.Y.; Hur, S.J. Antihypertensive peptides from animal products, marine organisms, and plants. *Food Chem.* **2017**, *228*, 506–517. [[CrossRef](#)] [[PubMed](#)]
26. Ferreira, A.J.; Shenoy, V.; Yamazato, Y.; Sriramula, S.; Francis, J.; Yuan, L.; Castellano, R.K.; Ostrov, D.A.; Oh, S.P.; Katovich, M.J. Evidence for angiotensin-converting enzyme 2 as a therapeutic target for the prevention of pulmonary hypertension. *Am. J. Respir. Crit. Care Med.* **2009**, *179*, 1048–1054. [[CrossRef](#)] [[PubMed](#)]
27. Hernández Prada, J.A.; Ferreira, A.J.; Katovich, M.J.; Shenoy, V.; Qi, Y.; Santos, R.A.; Castellano, R.K.; Lampkins, A.J.; Gubala, V.; Ostrov, D.A. Structure-based identification of small-molecule angiotensin-converting enzyme 2 activators as novel antihypertensive agents. *Hypertension* **2008**, *51*, 1312–1317. [[CrossRef](#)]
28. Chappell, M.C. Emerging evidence for a functional angiotensin-converting enzyme 2-angiotensin-(1-7)-MAS receptor axis: More than regulation of blood pressure? *Hypertension* **2007**, *50*, 596–599. [[CrossRef](#)]
29. Malayeri, A.A.; Natori, S.; Bahrami, H.; Bertoni, A.G.; Kronmal, R.; Lima, J.A.; Bluemke, D.A. Relation of aortic wall thickness and distensibility to cardiovascular risk factors (from the Multi-Ethnic Study of Atherosclerosis [MESA]). *Am. J. Cardiol.* **2008**, *102*, 491–496. [[CrossRef](#)]
30. Jin, C.-Z.; Nam, K.-H.; Paeng, D.-G. The spatio-temporal variation of rat carotid artery bifurcation by ultrasound imaging. In Proceedings of the 2014 IEEE International Ultrasonics Symposium, Chicago, IL, USA, 3–6 September 2014; IEEE: New York, NY, USA, 2014; pp. 1900–1903.